BIOCHEMISTRY
including biophysical chemistry & molecular biology

Rapid Report

pubs.acs.org/biochemistry

Revealing Cell-Surface Intramolecular Interactions in the BlaR1 Protein of Methicillin-Resistant *Staphylococcus aureus* by NMR Spectroscopy

Thomas E. Frederick, Brian D. Wilson, Jooyoung Cha, Shahriar Mobashery, and Jeffrey W. Peng*

The Department of Chemistry and Biochemistry, University of Notre Dame, Notre Dame, Indiana 46556, United States

Supporting Information

ABSTRACT: In methicillin-resistant *Staphylococcus aureus*, β-lactam antibiotic resistance is mediated by the transmembrane protein BlaR1. The antibiotic sensor domain BlaR^S and the L2 loop of BlaR1 are on the membrane surface. We used NMR to investigate interactions between BlaR^S and a water-soluble peptide from L2. This peptide binds BlaR^S proximal to the antibiotic acylation site as an amphipathic helix. Acylation of BlaR^S by penicillin G does not disrupt binding. These results suggest a signal transduction mechanism whereby the L2 helix, partially embedded in the membrane, propagates conformational changes caused by BlaR^S acylation through the membrane via transmembrane segments, leading to antibiotic resistance.

Methicillin-resistant *Staphylococcus aureus* (MRSA) is a global clinical scourge that has become resistant to virtually all β-lactam antibiotics. In many MRSA strains, the β-lactam resistance is induced by a transmembrane sensor/signal transducer protein, BlaR1 (Figure 1). The induction begins when the extracellular sensor domain of BlaR1, BlaR^S, becomes acylated at Ser389 by a β-lactam antibiotic. Transduction of this signal to the BlaR1 cytoplasmic domain leads to transcription and expression of antibiotic-resistance determinants.[1−3]

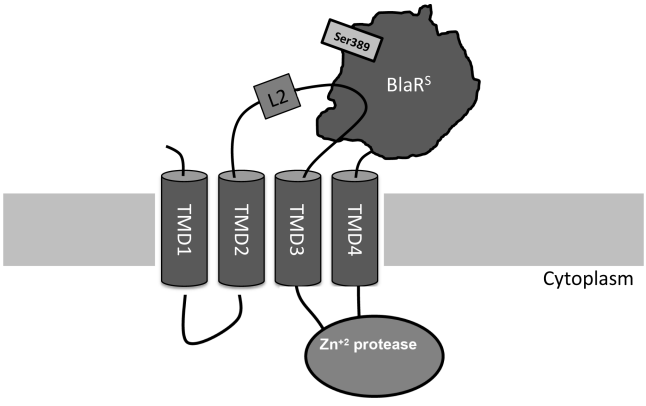

Figure 1. Arrangement of domains in the BlaR1 protein of methicillin-resistant *S. aureus*.

The initial events related to acylation are not fully understood. Previous studies of BlaR1 from *Bacillus licheniformis*[4] demonstrated an interaction between the aforementioned BlaR^S and extracellular transmembrane loop L2 (Figure 1). It is reasonable to hypothesize that this interaction plays a role in signal transduction. Herein, we describe studies that disclose the nature of the interactions between BlaR^S and the L2 loop and clarify the early events leading to transduction of the acylation signal through the membrane in *S. aureus*.

We investigated the BlaR^S−loop L2 interactions through solution NMR studies of the isolated sensor domain, BlaR^S (residues 330−585), and a peptide corresponding to the 33 C-terminal amino acids of loop L2 (residues 73−105). The full-length L2 peptide (residues 39−105) was insoluble; therefore, we used the soluble truncated construct, L2short, for all NMR experiments.

Backbone amide ^{15}N spin relaxation parameters [R_1, R_2, and heteronuclear nuclear Overhauser effect (NOE)] of [U-^{15}N]-L2short in the absence and presence of equimolar BlaR^S (300 μM) indicated L2short undergoes rapid exchange between a major free state and a minor BlaR^S-bound state (Supporting Information). From decreases in R_1, we estimated an equilibrium dissociation constant (K_d) of 1.3 ± 0.4 mM. In intact BlaR1, colocalization of L2short and BlaR^S on the membrane surface would impose a favorable entropic factor in their interactions that the millimolar K_d does not reflect. A reduced spectral density determination of L2short $J_{eff}(0)$ values suggested C-terminal residues 94−102 contact BlaR^S directly (Figure S1 of the Supporting Information).

Determining where L2short binds BlaR^S was of interest. Detecting intermolecular NOEs proved to be unsuccessful, most likely because of the weak binding affinity.[5,6] We therefore used paramagnetic relaxation enhancement (PRE) measurements, which are well suited for fast-exchange binding interactions.[7−9] Our PRE measurements reported herein directly established the location and binding mode of the L2short−BlaR^S interaction, which were inconclusive from chemical shift perturbations (CSPs), NOEs, and line broadening.

To take the PRE measurements, we generated a T92C variant of L2short and attached paramagnetic and diamagnetic moieties consisting of MTSL and acetyl-MTSL, respectively (Figure S2 of the Supporting Information). We chose T92 because of its proximity to the L2-binding interface residues

Received: November 19, 2013
Revised: December 19, 2013
Published: December 20, 2013

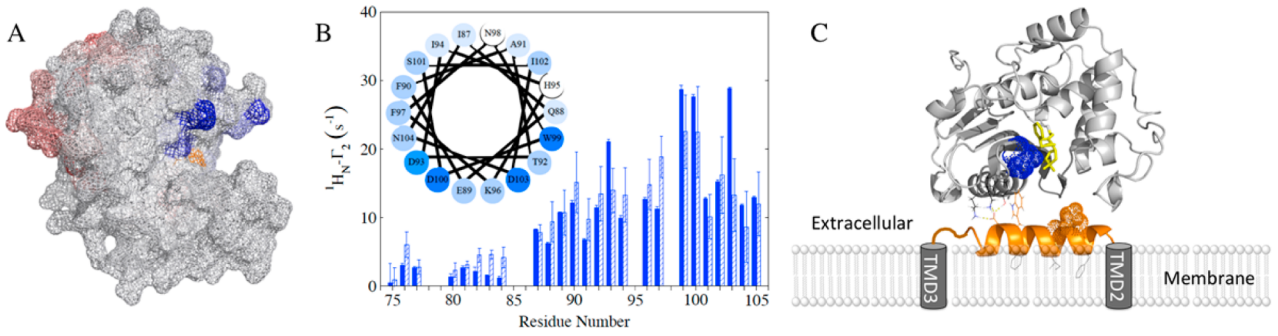

Figure 2. (A) BlaR^S PRE Γ_2 rates caused by spin-labeled L2short T92C mapped onto the BlaR^S crystal structure (Protein Data Bank entry 3Q7V, chain B). Blue ($\beta5-\beta6$ turn) and red ($\beta6-\beta7$ turn) indicate the two interaction regions. Darker shading indicates larger $^1H^N$ Γ_2 values. Antibiotic binding site residue S389 is colored orange. (B) L2short PRE $^1H^N$ Γ_2 rates caused by IAP-labeled BlaR^S I531C without (dark blue) and with (dashed) penicillin G. The helical wheel includes I87–N104 of L2short, with darker shading for higher $^1H^N$ Γ_2 rates. (C) Model for the interaction of loop L2 with BlaR^S, based on PREs from I531C (BlaR^S) and T92C (L2short), and CSPs from the $\beta5-\beta6$ turn. BlaR^S is colored gray. The L2short helix is colored orange. I531 is shown as blue spheres. The acylation site of BlaR^S is shown with penicillin G rendered with yellow sticks.

revealed by $J_{eff}(0)$ (Figure S1 of the Supporting Information). We then measured the amide proton transverse relaxation rates $R_2(^1H^N)$ of [U-^{15}N, 80% ^{2}D]BlaR^S in the presence of the paramagnetic and diamagnetic T92C variants. The PREs were the differences between the paramagnetic and diamagnetic $R_2(^1H^N)$ relaxation rates, namely, $\Gamma_2 = R_2^{PARA}(^1H^N) - R_2^{DIA}(^1H^N)$.[8,9] BlaR^S amide protons with large Γ_2 rates were sites that experienced greater electron–nuclear dipolar relaxation, indicating proximity to the L2short spin-label and, thus, involvement in the binding interface.

Two regions of BlaR^S gave significant PREs, suggesting two binding sites (Figure 2A). The first region (blue) was proximal to the antibiotic-binding site (site of acylation), which includes residues in the $\beta5-\beta6$ turn. The second region (red) was distal from the antibiotic-binding site and includes residues in the $\beta6-\beta7$ turn. The distal site PRE values were smaller, reflecting a different binding mode with larger intermolecular distances, a lower binding affinity, or both. Addition of L2short to [U-^{15}N, 80% ^{2}D]BlaR^S to final concentrations of 3 mM L2short and 300 μM BlaR^S resulted in BlaR^S CSPs that corroborated the PRE results (Figure S3 of the Supporting Information).

We corroborated these results from the L2short perspective, by spin-labeling BlaR^S and looking for amide proton PREs in [U-^{15}N]L2short. We made two BlaR^S variants for iodoacetamido-proxyl (IAP) (Figure S2 of the Supporting Information) spin-labeling: I531C and N548C. I531 lies within the proximal L2short binding site ($\beta5-\beta6$ turn), while N548 is within the distal L2short binding site ($\beta6-\beta7$ turn).

The L2short PREs highlighted the same C-terminal region (residues 94–102) as the ^{15}N $J_{eff}(0)$ results; thus, these L2short residues clearly contribute to the binding interface. The L2short PREs caused by I531C (Figure 2B) were significantly greater than those caused by N548C; this is consistent with converse PRE experiments involving T92C. Figure S4 of the Supporting Information compares the two PRE profiles.

The L2short PREs from I531C showed a distinct undulation for residues 87–104, which indicated cyclic proximity of these residues to spin-labeled I531C. The pattern was consistent with an amphipathic α-helix (Figure 2B). $^1H-^1H$ NOESY spectra of L2short in the presence of BlaR^S confirmed this α-helical model by giving the characteristic sequential $^1H^N-^1H^N$ NOEs (Figure S5 of the Supporting Information).[10]

Figure 2C depicts our provisional model of the L2short–BlaR^S binding mode at the proximal site; this was derived from HADDOCK[11] calculations using our PRE-derived intermolecular distances[12] and BlaR^S CSPs. The L2short residues in the binding interface are mainly in the polar hydrophilic face of the α-helix, with putative interactions between D100 of L2short and K535/K562 of BlaR^S. An exception is W99, which gave a very strong PRE. Hydrophobic interactions between W99 and BlaR^S residues I531 and Y536 may enhance binding. Otherwise, the hydrophobic patches on the helix are opposite the BlaR^S surface, allowing for partial embedding into the membrane (Figure 2C).

The binding mode for L2short at the BlaR^S distal interaction site was unclear. The smaller L2short PREs precluded assessment of a similar amphipathic α-helix. The mainly polar residues at the distal site suggest binding is dominated by electrostatic interactions. PRE experiments at higher salt concentrations supported this hypothesis. The higher salt concentration reduced the distal site PRE to near noise levels; by contrast, the proximal site PREs remained prominent, albeit, at a reduced level (Figure S3 of the Supporting Information). HADDOCK modeling deemed unlikely a scenario in which one L2short binds the proximal and distal sites simultaneously. Rather, L2short binds one or the other. The weaker PRE response and the lack of evidence of structured binding suggest the distal binding site reflects a nonspecific interaction.

A natural question is whether the α-helicity of L2short is induced upon binding BlaR^S. Far-UV circular dichroism (CD) measurements showed that isolated L2short is disordered in solution (Figure S6 of the Supporting Information), yet the same isolated L2short retained the α-helix NOE pattern[10] seen in the presence of BlaR^S (Figure S5 of the Supporting Information). These results are not contradictory: the r^{-6} distance dependence of the $^1H-^1H$ NOE is sensitive to sparsely populated conformers with short interproton distances,[13,14] such as that found within an α-helix. Together, the CD and NMR results suggest that the isolated L2short transiently samples the bound-state helix, which stabilizes upon binding BlaR^S (conformational selection).

Finally, we investigated the effect of β-lactam acylation of BlaR^S on the L2short interaction. For acylation, we added penicillin G (penG) to a 5-fold molar excess over BlaR^S. BlaR^S $^{15}N-^1H$ CSPs monitored during a penG titration indicated that this excess was sufficient for acylation throughout the experiment. We then introduced [U-^{15}N]L2short in a 1:1 ratio with the preacylated BlaR^S. Both ^{15}N relaxation (Figure S1

dx.doi.org/10.1021/bi401552j | Biochemistry 2014, 53, 10–12

of the Supporting Information) and PRE measurements for L2short (Figure S4 of the Supporting Information) showed only minimal changes compared to the unacylated complex. Thus, acylation of $BlaR^S$ by the antibiotic does not disrupt its interaction with L2short, as suggested previously.[4] However, residue-specific changes remain possible and are likely contributors of the signal transduction mechanism. This lack of disruption of the complex upon antibiotic binding is consistent with the L2short binding site being proximal to the acylation site, rather than occluding it.

In conclusion, our studies document the nature of the intramolecular interactions between L2 and the $BlaR^S$ sensor domain on the membrane surface, which are important for antibiotic recognition and signal transduction. $BlaR^S$ acylation by penG does not disrupt the interaction. The proximity of L2 to the membrane surface suggests that the amphipathic α-helix (Figure 2C) partially embeds itself into the membrane. Thus, we assert that L2−$BlaR^S$ interaction (i) helps anchor the sensor domain to the membrane surface and (ii) provides the means by which conformational perturbations in the sensor domain $BlaR^S$, resulting from its acylation, propagate through the membrane to initiate the events in the cytoplasm that lead to full-blown antibiotic resistance. This picture for the first time reveals the specific interactions and early events on the membrane surface of MRSA required for signaling from the cell exterior to the cytoplasm.

■ ASSOCIATED CONTENT

Supporting Information

Materials and methods for all experiments and supporting Figures S1−S6. This material is available free of charge via the Internet at http://pubs.acs.org.

■ AUTHOR INFORMATION

Corresponding Author

*E-mail: jpeng@nd.edu. Phone: (574) 631-2983.

Funding

This work was supported by National Institutes of Health Grants AI104987 (to S.M.) and GM085109 (to J.W.P.).

Notes

The authors declare no competing financial interest.

■ ACKNOWLEDGMENTS

We thank Dr. Leticia Llarrull, Mr. Michael Staude, Dr. Xingsheng Wang, Dr. Mandy Blackburn, and Dr. Gail Fanucci for valuable discussions.

■ REFERENCES

(1) Llarrull, L. I., Fisher, J. F., and Mobashery, S. (2009) *Antimicrob. Agents Chemother. 53*, 4051−4063.
(2) Llarrull, L. I., Toth, M., Champion, M. M., and Mobashery, S. (2011) *J. Biol. Chem. 286*, 38148−38158.
(3) Llarrull, L. I., and Mobashery, S. (2012) *Biochemistry 51*, 4642−4649.
(4) Hanique, S., Colombo, M. L., Goormaghtigh, E., Soumillion, P., Frere, J. M., and Joris, B. (2004) *J. Biol. Chem. 279*, 14264−14272.
(5) Zuiderweg, E. R. (2002) *Biochemistry 41*, 1−7.
(6) Peng, J. W., Moore, J. M., and Abdul-Manan, N. (2004) *Prog. Nucl. Magn. Reson. Spectrosc. 44*, 225−256.
(7) Jahnke, W., Rüdisser, S., and Zurini, M. (2001) *J. Am. Chem. Soc. 123*, 3149−3150.
(8) Clore, G. M., and Iwahara, J. (2009) *Chem. Rev. 109*, 4108−4139.
(9) Iwahara, J., and Clore, G. M. (2006) *Nature 440*, 1227−1230.
(10) Wagner, G. (1990) *Prog. Nucl. Magn. Reson. Spectrosc. 22*, 101−139.
(11) de Vries, S. J., van Dijk, M., and Bonvin, A. M. (2010) *Nat. Protoc. 5*, 883−897.
(12) Battiste, J. L., and Wagner, G. (2000) *Biochemistry 39*, 5355−5365.
(13) Bruschweiler, R., Blackledge, M., and Ernst, R. R. (1991) *J. Biomol. NMR 1*, 3−11.
(14) Bonvin, A. M., Boelens, R., and Kaptein, R. (1994) *J. Biomol. NMR 4*, 143−149.